Evaluation of different methods for measuring the impedance of Lithium-ion batteries during ageing

Stroe, Daniel Loan; Swierczynski, Maciej Jozef; Stroe, Ana-Irina; Knap, Václav; Teodorescu, Remus; Andreasen, Søren Juhl

Published in:
Proceedings of the 2015 Tenth International Conference on Ecological Vehicles and Renewable Energies (EVER)

DOI (link to publication from Publisher):
10.1109/EVER.2015.7113024

Publication date:
2015

Document Version
Accepted author manuscript, peer reviewed version

2015 Tenth International Conference on Ecological Vehicles and Renewable Energies (EVER)

Evaluation of Different Methods for Measuring the Impedance of Lithium-Ion Batteries during Ageing

Daniel-Ioan Stroe, Maciej Swierczynski, Ana-Irina Stroe, Vaclav Knap, Remus Teodorescu, Søren J. Andreasen
Department of Energy Technology, Aalborg University
Pontoppidanstræde 101, 9220 Aalborg, Denmark
Email: dis@et.aau.dk

***Abstract*—The impedance represents one of the most important performance parameters of the Lithium-ion batteries since it used for power capability calculations, battery pack and system design, cooling system design and also for state-of-health estimation. In the literature, different approaches are presented for measuring the impedance of Lithium-ion batteries and electrochemical impedance spectroscopy and dc current pulses are the most used ones; each of these approaches has its own advantages and drawbacks. The goal of this paper is to investigate which of the most encountered impedance measurement approaches is the most suitable for measuring the impedance of Lithium-ion batteries during ageing.**

Keywords— Lithium-Ion Battery, Impedance, Experimental, Ageing, Evaluation.

I. INTRODUCTION

Lithium-ion (Li-ion) batteries are characterized by outstanding properties in comparison to other energy storage technologies (e.g. supercapacitors, lead-acid and nickel-metal hybrid batteries, flow batteries) such as: high operating voltage (3.7 V in average), high gravimetric and volumetric energy densities, long calendar and cycle lifetime, and low self-discharge rate [1], [2]. Thus, the Li-ion batteries have become the energy storage technology to choose for many applications, including electric vehicles, grid support services, renewables' integration and back-up power applications [3]–[5].

On the other hand, Li-ion batteries are non-linear systems and their performance parameters, i.e. capacity and internal resistance, are highly dependent on the operating conditions. Thus, in order to maximize the energy efficiency and lifetime and to benefit from the aforementioned properties of the Li-ion batteries, accurate information about the capacity and internal resistance are required. Opposite to the battery's capacity, which can be measured easily, by integrating the current, the internal resistance is determined from the measured values for the voltage and current.

Precise knowledge of the internal resistance allows for determining the power capability of the Li-ion battery cell. Thus, by knowing the power capability of a battery cell, battery packs can be designed in order to meet the requirements of the targeted application. Furthermore, accurate knowledge of the internal resistance values over the whole battery's state-of-charge (SOC) interval allows for determining the SOC range, where the Li-ion battery cell operates with high efficiency. Finally, knowing the value of the internal resistance (and subsequently of the power capability) at every operating point during its lifetime will permit the battery management system to control the operation of the battery in an optimal way; thus, the lifetime of the Li-ion battery will be maximized and safety concerns will be mitigated.

The internal resistance, further referred as impedance (it is better to talk about impedance rather than resistance since the response of the battery cell to load changes is not like a pure resistor but is more complex and closer to R-C and R-L elements depending on the frequency), of Li-ion batteries varies significantly with the batteries' SOC, load current and temperature [6]-[8]. Moreover, the impedance of Li-ion batteries changes in time, mainly increasing, while the battery is ageing [9], [10]. Additionally, as illustrated in [9], the dependence trend of the impedance on parameters such as SOC and load current may change with ageing too.

Another aspect, which makes the measurement of the impedance of Li-ion batteries not a straightforward task, is represented by the variety of available measurement approaches; as presented in [11], the values of the impedance are varying dependent on the applied measurement approach. Therefore, the goal of this work is to investigate and evaluate, which impedance measurement approach brings the most meaningful results when it is used to measure the impedance of Li-ion batteries during ageing.

The paper is structured as follows: Chapter 2 presents a brief theoretical background of the two most used approaches to measure the impedance of Li-ion batteries. Chapter 3 gives an overview of the experimental setup, detailing the conditions used during the ageing tests and as well the test conditions during the impedance measurements. Chapter 4 presents the results obtained when the impedance of the Li-ion cell was measured following different approaches, during ageing. Chapter 5 evaluates which measurement approach is most suitable to measure the impedance of Li-ion batteries during ageing. Finally, Chapter 6 concludes the paper.

II. IMPEDANCE MEASUREMENT TECHNIQUES

A comprehensive review of different approaches to measure the impedance of Li-ion batteries is presented in [11]; however, in the aforementioned research, the different measurement approaches were applied only to a fresh cell. Thus, this work aims to go one step further and analyze and evaluate which of the two most used impedance measurement techniques, electrochemical impedance spectroscopy (EIS) and DC current pulses, is more suitable to measure the impedance of Li-ion batteries during their calendar and cycling ageing.

A. *Electrochemical Impedance Spectroscopy*

EIS represents a powerful measurement technique used mainly to characterize and model the dynamic behavior of Li-ion batteries [6]. For a detailed presentation of this measurement technique, the reader is referred to [12]. The result of the EIS measurement is represented by an impedance spectrum that is usually presented in the shape of a Nyquist plot, as illustrated in Fig. 1.

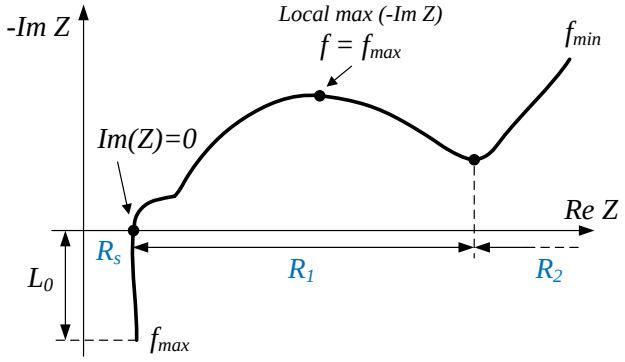

Fig. 1: Typical impedance spectra of a Li-ion battery cell

In order to analyze, the results obtained from the EIS measurement, the impedance spectra of the Li-ion battery cell is fitted using an equivalent electrical circuit (EEC). If an appropriate EEC is chosen, the impedance spectra can be decomposed into contributions from various processes, which take places inside the battery cell with different time constants. Furthermore, these contributions can be linked to the different parameters of the EEC, for example: R_s with the ohmic resistance, R_1 with the charge transfer resistance and R_2 with the diffusion process. In this work, the measured impedance spectra of the tested Li-ion battery cells have been curve fitted using the equivalent electrical circuit (EEC) presented in Fig. 2.

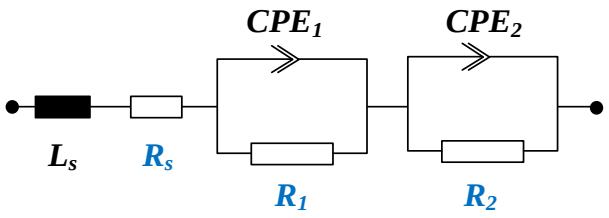

Fig. 2: EEC used to fit the impedance spectra measured during both cycling and calendar ageing.

Because the impedance spectra of the Li-ion batteries is changing with the ageing, the parameters of the EEC are changing as well during the degradation of the cell; however, due to the goal of this work, only the variation with ageing of the resistances R_s, R_1, R_2 of the EEC will be analyzed, while the other parameters will be disregarded.

In comparison with other impedance measurement approaches (i.e. DC current pulses), during the EIS measurement, the SOC of the Li-ion battery cell is no changing if the measurements is performed without superimposed DC current. On the other hand, this impedance measurement approach is time consuming (impedance measurement at low frequencies are long) and requires additional testing equipment (i.e. impedance spectroscopy analyzer).

Other researchers have used as well the EIS technique to measure the impedance of Li-ion battery cells during ageing [10], [13], [14]; however, in none of these works, the impedance increasing trends obtained from the EIS measurement approach were not compared with the impedance increase trends obtained with other impedance measurement approaches.

B. *DC Current Pulses*

The DC Current pulse approach is the most used method to measure the impedance of Li-ion battery cells. Moreover, this method is usually used to determine the cell's impedance during ageing (calendar or cycling) and thus to evaluate the degradation of the Li-ion battery cells.

The measurement approach is straightforward and consists of applying a current pulse (ΔI) to the cell and measuring the resulting change in the voltage (ΔV); the impedance of the battery (R) is obtained by dividing the voltage change by the current as given in (1). The obtained value is mostly used for power capability calculation and state-of-health estimation.

$$R = \frac{\Delta V}{\Delta I} = \frac{V_1 - V_0}{I_1 - I_0} \tag{1}$$

When measuring the impedance of Li-ion batteries with the DC current pulse approach, two methods can be distinguished:

- The current injection method, when the resistance is determined during the current pulse;
- The current interruption method, when the resistance is determined after the current pulse is cut-off.

Usually, the values of the impedance obtained with the current injection method are slightly higher compared to the values obtained with the current interruption method; this difference is caused mainly by the diffusion polarization [8]; however, this difference can be mitigated by allowing a long relaxation time after the cut-off of the current, which will allow the equilibrium to be established [8].

Similar to the case of the EIS approach, the values of the impedance measured by the DC current pulse method are sensitive to the temperature and SOC. Moreover, independent on the applied method (i.e. current injection or current interruption), the obtained impedance is influenced by the pulse length and by its amplitude; the obtained resistance is increasing by increasing the pulse duration [8] and [11]. On the other hand, for the effect of the pulse amplitude on the value of the

impedance, different researchers are reporting opposite effects: in [8], it is reported that the impedance decreases with increasing the pulse magnitude, while in [11] it is shown that the impedance decreases with decreasing the pulse magnitude.

One disadvantage of the current injection method is represented by the fact that during the DC current pulse, the SOC of the battery cell can modify significantly (depending on the current's amplitude and length) and thus the value of the measured impedance for the corresponding SOC is altered. This issue can be mitigated if the current interruption method is used, since the influence of the SOC change during the measurement is eliminated; however, when this method is used the impedance of the Li-ion battery cell is not measured at the desired SOC level but at the SOC level measured at the end of the current pulse [11]. The aforementioned issue can be disregarded for the Li-ion cell's chemistries which are characterized by a flat voltage curve, as is the case of the lithium iron phosphate chemistry.

The choice of the second voltage point for calculating the impedance using the current interruption method is relatively arbitrary. For example Smart et al. in [15], are determining the impedance of the battery cell after two hours, while Ecker et al. [10], are computing the impedance after 40 seconds.

In this work, the impedance of the tested Li-ion cell was computed with the current interrupt method after 40 seconds from the cut-off of the current, as it is mentioned in [16]. With the current injection method, the impedance of the tested battery cell was determined after 2, 10, and 18 seconds [16]; the voltage and current profiles during the measurement are illustrated in Fig. 3.

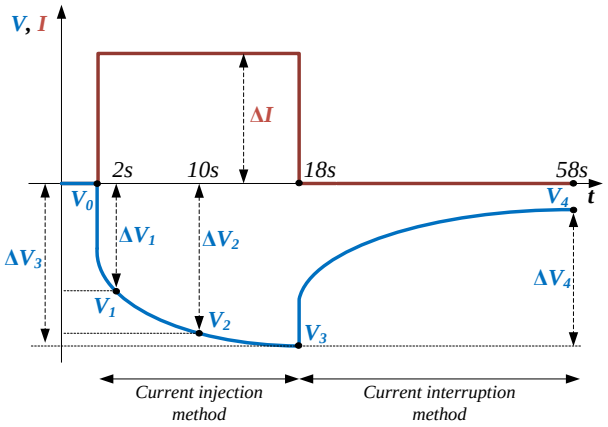

Fig. 3: Current (red) and voltage (blue) profiles during impedance measurement with the DC current pulse approach

The 2 seconds discharge impedance, R_{2s}, the 10 seconds discharge impedance, R_{10s}, and the 18 seconds discharge impedance, R_{18s}, determined with the current injection method, were computed according to (2) - (4) respectively. While the overall discharge impedance, R_{40s} determined with the current interruption method was computed according to (5).

$$R_{2s} = \frac{\Delta V_1}{\Delta I} = \left|\frac{V_1 - V_0}{I_1 - I_0}\right| \quad (2)$$

$$R_{10s} = \frac{\Delta V_2}{\Delta I} = \left|\frac{V_2 - V_0}{I_1 - I_0}\right| \quad (3)$$

$$R_{18s} = \frac{\Delta V_3}{\Delta I} = \left|\frac{V_3 - V_0}{I_1 - I_0}\right| \quad (4)$$

$$R_{40s} = \frac{\Delta V_4}{\Delta I} = \left|\frac{V_4 - V_3}{I_1 - I_0}\right| \quad (5)$$

Where, V_0 is the open-circuit voltage, measured before applying the current pulse, V_1 is the voltage measured after 2 seconds, V_2 is the voltage measured after 10 seconds, V_3 is the voltage measured after 18 seconds, V_4 is the voltage measured after 40 seconds from the cut-off of the current, I_0 is the current measured after applying and cutting off the current, and I_1 is the current measured during the pulse.

III. Experimental Setup and Methodology

A. Li-ion battery cell under test

Nanophosphate-$LiFePO_4$/C battery cells with a capacity of 2.5Ah have been used to perform the present evaluation. Battery cells with the same chemistry are used in both electrical vehicles and stationary applications.

For each of the two ageing tests considered in this work, three nanophosphate-$LiFePO_4$/C cells were considered; thus, the effect of possible battery cells outliers on the obtained results was minimized. Moreover, the impedance values presented in *Section IV* are the average values obtained for the three cells tested under similar conditions.

B. Accelerated Ageing Tests

The impedance of the Li-ion batteries is increasing during both storage (calendar ageing) and charging/discharging (cycling ageing). Therefore, in order to have a complete overview of which measurement techniques is more suitable to measure the impedance of the $LiFePO_4$/C battery cells during ageing both calendar and cycling ageing tests were performed.

Because the lifetime of the tested nanophosphate-LiFePO4/C battery cells is in the range of years, if they are tested at normal operating conditions, accelerated calendar and cycling ageing tests were performed; the calendar ageing was accelerated by using a high temperature, while the cycling ageing was accelerated by using a high temperature and a high symmetrical charging-discharging current rate. The ageing conditions for the two different tests are summarized in Table I.

TABLE I. Accelerated Ageing Conditions

Test	Stress factor and stress level			
	Temperature	*SOC-level*	*Cycle depth*	*Current*
Calendar	40°C	50%	–	–
Cycling	42.5°C	50%	60%	10A (4C-rate)

C. Impedance Measurements

All the impedance measurements were performed in a climatic chamber, at 25°C; prior to the measurement a 15 minutes relaxation time was considered. Moreover, the impedance of the tested battery cells was measured at three

different SOC levels (i.e. low, medium, and high SOC-level); however, in this evaluation, only the results measured at high SOC-level (i.e. (80%) were considered since this SOC is representative for all the applications, which can be covered by Li-ion batteries: EVs, grid support, and back-up power supply.

The impedance of the tested battery cells was measured at the beginning of life (BOL) and periodically thereafter at specific time intervals: one month for cells aged under calendar conditions and 550 cycles (approximately one week) for cells aged under cycling conditions.

The impedance of the tested battery cells measured using the EIS technique was performed in the galvanostatic mode, using a sweep of 50 frequency points in the interval 10 kHz – 10 mHz. Whereas, the impedance of the battery cells measured using the DC current approach was obtained by applying a 10A current pulse for 18 seconds similar as presented in [16].

IV. Results

A. Impedance at beginning of life

The impedance values of the tested nanophosphate-LiFePO4/C battery cells, which were measured at BOL, are summarized in Table II.

TABLE II. Comparison of the Impedance Values Measured with Different Techniques (T=25°C, SOC=80%)

Technique	Impedance notation	Impedance value [mΩ]	
		Cell for calendar ageing	*Cell for cycling ageing*
Current injection	2 seconds pulse, R_{2s}	9.4	8.9
	10 seconds pulse, R_{10s}	12.6	12.13
	18 seconds pulse, R_{18s}	13.9	13.5
Current interuption	40 seconds interrupt. R_{40s}	12.2	11.67
EIS	Series resistance, R_s	5.27	5.04
	Resistance R_2	42.15	46.04

By applying the DC current pulse techniques, impedance values in the range of 9 to 13 mΩ have been measured. The impedance values obtained with the current interruption technique are very similar to the ones measured with the current injection technique suggesting that this impedance measurement technique might be used for power capability calculations. The difference in the measured impedance values with the DC current pulse techniques between the cells considered for calendar and cycling ageing were considered to be cause mainly by the battery cell manufacturing tolerances.

The impedance values, obtained by applying the EIS techniques are different than the ones measured with the DC pulse techniques. Moreover, because they are small signal impedances, these impedances (i.e., R_s and R_2) are usually not used for power capability calculations; however, it has to be highlighted that some correlations between the impedance measured by EIS techniques and power capability determined by DC pulse technique were reported in literature [14], [17].

B. Impedance increase – calendar ageing

1) DC Current Pulse Technique

The effect of the calendar ageing on the voltage drop observed during the impedance measurement with the current injection and current interruption methods is illustrated in Fig. 4. Even though the impedance measurements were performed after each month of accelerated ageing, for a better visualization and interpretation of the results, a four months resolution was considered.

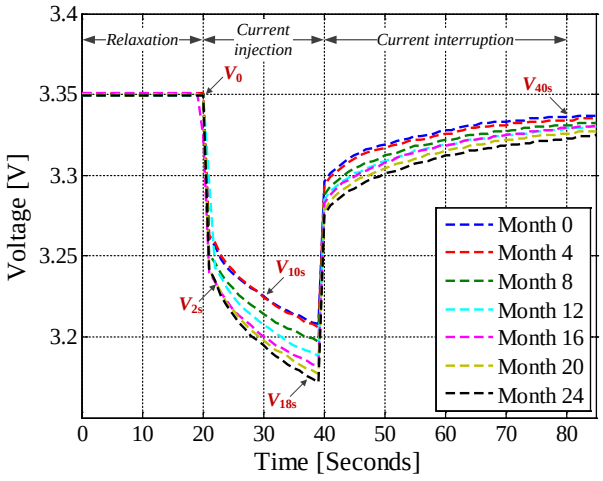

Fig. 4: Effect of the accelerated calendar ageing on the voltage behavior of the battery cell during current injection and current interruption

Based on the voltage profiles illustrated in Fig. 3 and on the impedance calculations formulas (2) – (5), the targeted battery impedances were calculated after each month of calendar ageing. Furthermore, in order to analyze the impedance increase, which was caused by the induced ageing process, the impedance values measured after each month were related to the value measured at the cells' beginning of life (BOL); the obtained results for the four considered impedances are shown in Fig. 5.

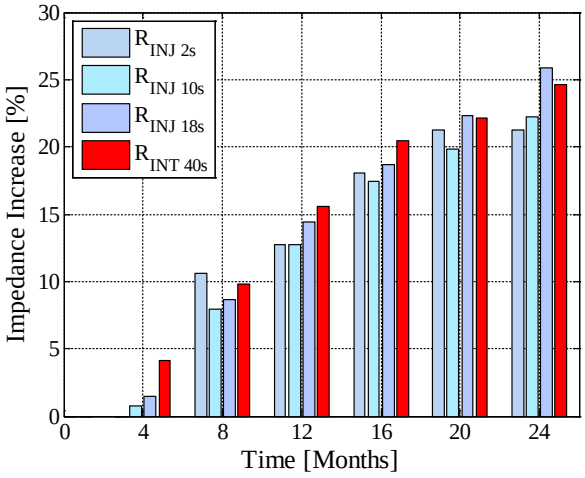

Fig. 5: Comparison between the increase of the impedance (caused by calendar ageing) when different DC current pulse techniques were used.

As illustrated in Fig. 5, very similar impedance increase patterns were obtained independent on the technique used to measure the impedance of the nanophosphate-$LiFePO_4$/C battery cells; this behavior is also presented in Table III, where the impedance increase was expressed as function of the storage time using the power law (6). Furthermore, it has to be highlighted that the obtained impedance increase values, for the four different impedance measurement approaches, are varying in a narrow interval (i.e., 3-4%) during the whole ageing process.

$$Z_{increase} = a_t \cdot t^{b_t} \quad (6)$$

Where, $Z_{increase}$ represents the increase of the impedance measured with each of the four approaches, t represents the storage time expressed in months, a_t and b_t represents the coefficient and the exponent of the power law function.

TABLE III. ESTIMATED IMPEDANCE INCREASE DURING CALENDAR AGEING (IMPEDANCE MEASURED WITH THE DC PULSE TECHNIQUE)

Estimation	Accuracy
$R_{2s\_increase} = 0.8939 \cdot t^{1.04}$	$R^2 = 0.9228$
$R_{10s\_increase} = 0.8728 \cdot t^{1.04}$	$R^2 = 0.9673$
$R_{18s\_increase} = 0.9854 \cdot t^{1.04}$	$R^2 = 0.9814$
$R_{40s\_increase} = 1.8530 \cdot t^{0.830}$	$R^2 = 0.9811$

2) *EIS technique*

The impedance spectra of the nanophosphate-$LiFePO_4$ battery cell, measured at different state of health (SOH) levels, during calendar ageing, are illustrated in Fig. 6; all the EIS measurements were performed for the frequency interval 10 kHz – 10 mHz. In order to allow for a good comparison between the results obtained using the two different impedance measurement techniques (i.e. EIS and DC pulses), the results obtained at similar time instants (i.e. number of months for calendar ageing) are presented; the same approach was followed for the cycling ageing case also, as presented in Section IV.C.

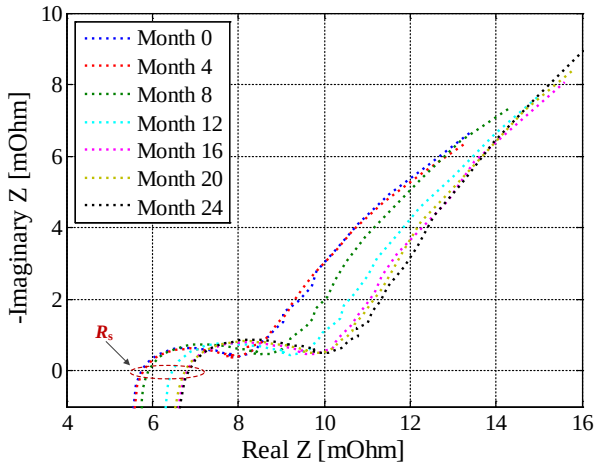

Fig. 6: Impedance spectra of the nanophospate-$LiFePO_4$ measured at different SOH levels during calendar ageing

Based on a complex non-linear least square (CNLS) algorithm, the impedance spectra which have been measured throughout the considered accelerated ageing process, were curve fitted using the EEC shown in Fig. 2. During the CNLS algorithm, both real and imaginary components of the measured impedance are simultaneously fitted in the least square minimization.

In order to analyze the ageing behavior of the resistances R_s, R_1, and R_2 of the EEC, the values, which had been measured throughout the considered ageing processes, were related to the values measured at BOL. The results obtained for the resistance R_1 of the EEC have shown a large scattering over time and consequently, they were not considered for further analysis. The obtained ageing behavior for impedance components R_s and R_2 are illustrated in Fig. 7.

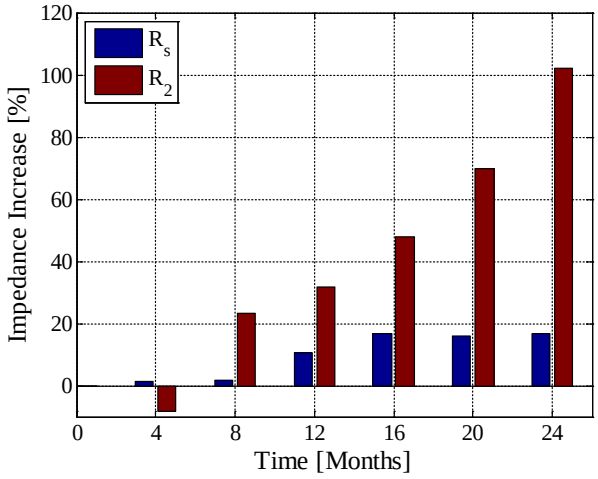

Fig. 7: Increase of the components of the AC impedance caused by calendar ageing

Both impedance components, R_s and R_2, have increased during the considered calendar ageing as shown in Fig. 7; however, the rate of increase of R_2 is much higher than the one of R_s. Moreover, the ageing patterns followed by the two investigated impedance components could be expressed with the same power law function (6) (see Table IV) that was also for the DC current pulse technique; nevertheless, in this case, lower accuracy estimation was obtained.

TABLE IV. ESTIMATED IMPEDANCE INCREASE DURING CALENDAR AGEING (IMPEDANCE MEASURED WITH THE EIS TECHNIQUE)

Estimation	Accuracy
$R_{s\_increase} = 0.5776 \cdot t^{1.103}$	$R^2 = 0.8734$
$R_{2\_increase} = 0.3857 \cdot t^{1.749}$	$R^2 = 0.9719$

C. *Impedance increase – cycling ageing*

The impedance increase of the tested nanophosphate-$LiFePO_4$ battery cells, which was caused by the cycling ageing conditions summarized in Table I, was analyzed following the same procedure as for the case of calendar ageing.

1) DC Current Pulse Technique

The voltage profiles registered during the battery cell impedance measurement with the current injection and interruption techniques at different SOH levels are presented in Fig. 8. The number of cycles values shown in Fig. 8 refer to cycles at the conditions listed in Table I and not to full cycles.

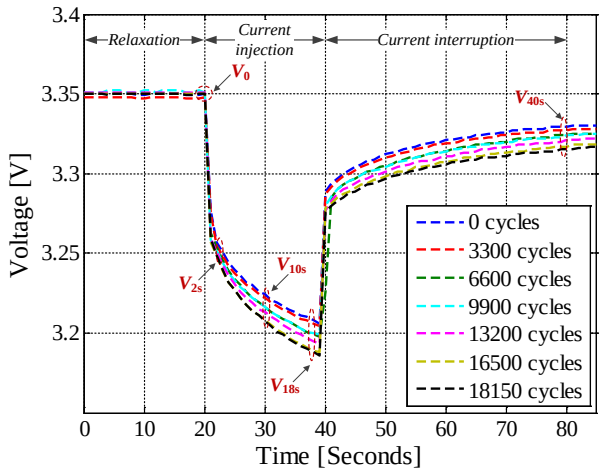

Fig. 8: Effect of the accelerated cycling ageing on the voltage behavior of the battery cell during current injection and current interruption

Based on the voltage profiles presented in Fig. 8 and formulas (2) – (5), the impedance values were calculated for both current injection and current interruption approaches. Following the same procedure as in the case of calendar ageing, to analyze the ageing behavior of the four considered impedances, the impedance values measured throughout the considered cycling ageing process were related to the impedance values measured at BOL, which are listed in Table II. A comparison between the impedance increase behaviors, obtained for the four calculated impedances, is presented in Fig. 9.

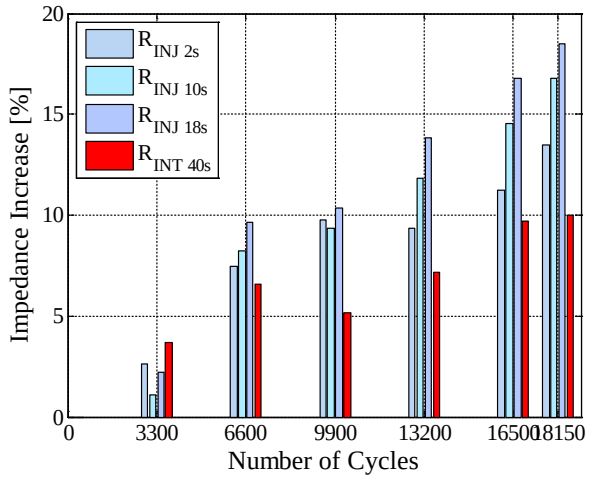

Fig. 9: Comparison between the increase of the impedance (caused by calendar ageing) when different DC current pulse techniques were used.

Similar ageing patterns were obtained for the impedances that were measured with the three current injection approaches. On the contrary, the trend of the impedance increase obtained for the case when the battery cell impedance was measured with the current interruption method is not straightforward. Furthermore, the impedance increase rate obtained for the current interruption method is lower than the rate of impedance increased obtained for the current injection methods. These aspects are also highlighted in Table V where the measured impedance increase is expressed as function of number of cycles (*nc*) using the power law (6), which was proposed also in the case of impedance increase caused by calendar ageing.

TABLE V. ESTIMATED IMPEDANCE INCREASE DURING CYCLING AGEING (IMPEDANCE MEASURED WITH THE DC PULSE TECHNIQUE)

Estimation	**Accuracy**
$R_{2s\_increase} = 0.00322 \cdot nc^{0.85}$	$R^2 = 0.9378$
$R_{10s\_increase} = 0.00385 \cdot nc^{0.85}$	$R^2 = 0.9587$
$R_{18s\_increase} = 0.00439 \cdot nc^{0.85}$	$R^2 = 0.9719$
$R_{40s\_increase} = 0.03034 \cdot nc^{0.587}$	$R^2 = 0.9265$

2) EIS Technique

Figure 10 presents the impedance spectra of the nanophosphate-$LiFePO_4$ battery cell, measured at different SOH levels, during cycling ageing. The measured EIS curves were fitted using the EEC presented in Fig. 2 and the impedance components R_s, R_1, and R_2 were extracted.

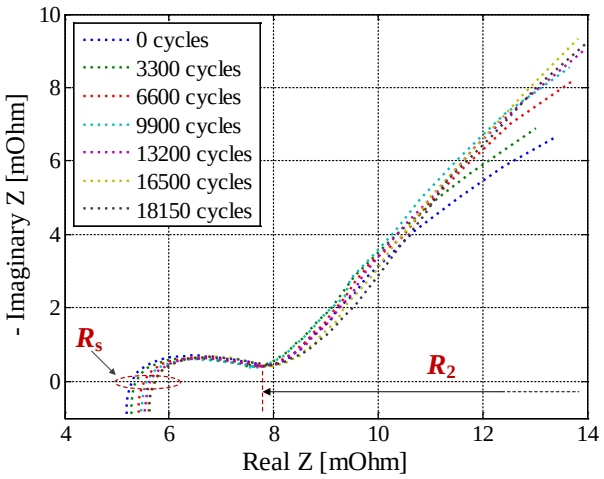

Fig. 10: Impedance spectra of the nanophospate-$LiFePO_4$ measured at different SOH levels during cycling ageing

In order to determine the ageing behavior of the three resistive components of the impedance spectra, their measured values throughout the cycling ageing process have been related to the values measured at BOL. Likewise the case of the calendar ageing, the ageing trend of resistance R_1 has shown a large scattering over time and this parameter was not considered for further evaluation. The ageing trends of the impedance components R_s and R_2, which were generated by cycling ageing, are illustrated in Fig. 11. Both impedance components increased

during the considered cycling ageing test. However, contrary to the case of the calendar ageing, the increase of R_s and R_2 is following different patterns. In the case of the impedance component R_s the impedance increase trend tends to slow down while the cycling ageing evolves, while in the case of the impedance component R_2, the impedance increase trend accelerates once the cycling ageing evolves. These different ageing behaviors are also highlighted in Table VI, where the dependence of the impedance increase on the number of cycles is expressed; to relate the impedance increase with the number of cycles, the same power law function (6) was used.

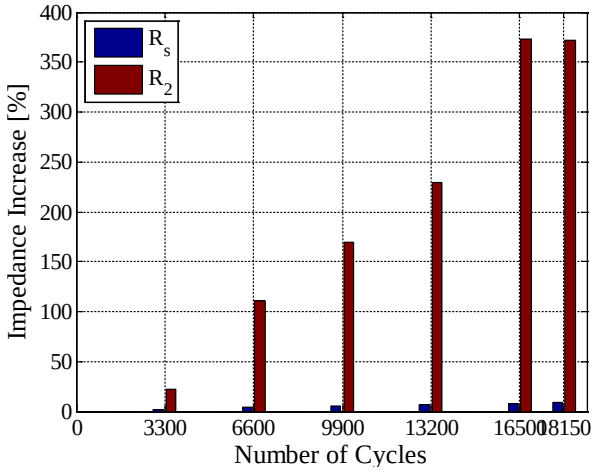

Fig. 11: Increase of the components of the AC impedance caused by calendar ageing

TABLE VI. ESTIMATED IMPEDANCE INCREASE DURING CYCLING AGEING (IMPEDANCE MEASURED WITH THE EIS TECHNIQUE)

Estimation	**Accuracy**
$R_{s\_increase} = 0.004282 \cdot nc^{0.7723}$	$R^2 = 0.9931$
$R_{2\_increase} = 0.000496 \cdot nc^{1.384}$	$R^2 = 0.9846$

V. DISCUSSON

In order to determine which of the presented approaches for measuring the impedance of Li-ion batteries is more suitable to be applied for measuring the impedance during ageing, five dimensions were considered: *complexity*, *time duration*, *estimation accuracy*, *power capability*, and *state change*. The *complexity* and *time duration* dimensions refer at the complexity and the duration of the applied measurement approach, respectively. The *estimation accuracy* dimension refers to the estimation accuracy of the impedance increase using the considered power law function (6). The *power capability* dimension refers to the possibility of using the measured impedance (with a certain method) to estimate the power capability of the battery cell. Finally, the *state change* dimension evaluates if the state of the battery was changed during the measurement of the impedance with a specific impedance measurement approach.

Because the three impedances measured with the current injection technique (R_{2s}, R_{10s}, and R_{18s}) had close values at the BOL and had followed very similar ageing patterns for calendar and cycling ageing, respectively, they will be evaluated together as a single method for impedance measurement during ageing. Furthermore, the use of the EIS technique for impedance measurement during ageing was evaluated considering the results obtained for both considered components of the impedance (i.e., R_s and R_2).

From the complexity point of view, the DC current pulse techniques are straightforward and are able to be performed without specialized battery testing equipment. On the other hand, the measurement of the Li-ion battery impedance with the EIS technique requires specialized laboratory equipment, which in most of the cases is expensive. Moreover, the accuracy of the impedance determination with the EIS technique depends also on the correct selection of the EEC used to fit the measured impedance spectrum and on the reliability of the applied fitting procedure.

The time duration of the impedance measurement with the DC current pulse techniques is less demanding than in the case when the EIS technique is used; the time duration of the EIS measurement is highly influence by the number of selected frequency points and by the value of the minimum frequency used for the frequency sweep. Consequently, an alternative solution would be to measure the Li-ion battery impedance only at high frequencies and determine only the R_s component of the impedance characteristic. This solution would be extremely suitable if the battery impedance would be used as an ageing diagnosis tool or for SOH determination and not for modelling the performance (dynamic) behavior of the battery cell.

An important advantage of the EIS technique over the current injection technique is the fact that during the impedance measurement with the first technique the state change (e.g. SOC, temperature etc.) of the battery cells is not changed if the EIS measurement is performed without superimposed DC current (i.e. without DC offset). In the case of the current interruption method, the SOC of the battery cell is not changed during the measurement; however, the impedance is not measured at the desired SOC level but at the SOC level measured at the end of the current pulse.

According to the existent battery testing standards, only the impedance measurement with the current injection method is suitable for determining the power capability of the Li-ion batteries [16]. On the other hand, as already mentioned, the use of the EIS technique for power capability determination was reported in literature [14], [17]. Nevertheless, there exist no general formulas, which can be used to directly derive the power capability value from the impedance measured with the EIS technique.

The power law function (6) was found to estimate accurately the ageing behavior of the impedance, measured with either investigated measurement techniques. However, in the case of the results obtained for the EIS technique, the ageing patterns are not all the time following clear trends (might be caused by the sensitivity of the measurement and by the curve fitting process) and can differ significantly depending on the impedance component investigated (i.e. R_s, R_1, and R_2). Moreover, based on the ageing results, summarized throughout Table III – Table VI, the impedance measured with either

techniques can be used to perform online SOH estimation of the battery cells; nonetheless, it has to be highlighted that in order to perform online SOH estimation/prediction using the EIS technique, additional devices (e.g., EIS analyzer) must be installed into the battery management system.

The comparison of the investigated impedance measurement methods from the five perspectives is graphically summarized in Fig. 12. The three impedance measurement methods (and the corresponding results) were compared relatively to each other; a result closer to the edge of the radar plot suggests a better suitability of a certain method from the considered perspective (e.g. complexity, time duration etc.).

As it can be observed from this figure none of the methods is better than the other two from all perspectives; however, the current injection technique resulted the most suitable method for measurement of the impedance of the tested nanophosphate-$LiFePO_4$/C during ageing.

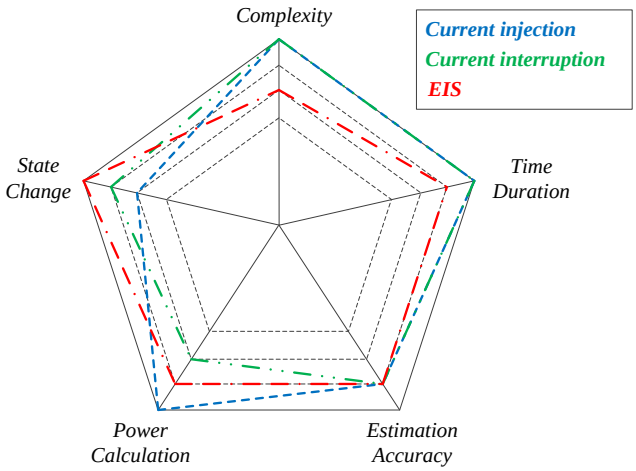

Fig. 12: Comparison of different Li-ion battery cell impedance measurement methods during ageing

VI. Conclusion

In this paper the suitability of different methods to measure the impedance of Li-ion batteries during ageing was evaluated. In order to perform this evaluation, both accelerated calendar and cycling ageing tests were performed in laboratory conditions. The impedance of the tested nanophosphate-$LiFePO_4$ battery cells was measured at the BOL and periodically thereafter with different approached: EIS, current injection and current interruption. By comparing the features of these measurement approaches along five dimensions, it was conclude that the current injection method is the most suitable approach to measure the impedance of the tested nanophosphate-$LiFePO_4$ battery cells during ageing.

Even though some of the results presented in this work might change depending on the chemistry of the Li-ion battery cell, the ageing tendencies, guidelines and conclusions derived from the presented results could apply to other Li-ion battery chemistries.

References

[1] G. Pistoia ed., “Lithium-Ion batteries. Advances and applications,” Elsevier, 2014, ISBN 978-0-444-59513-3.

[2] B. Dunn, H. Kamath, and J.-M. Tarascon, “Electrical energy storage for the grid: A battery of choices,” Science, vol. 334, pp. 928–935, 2011.

[3] A.I. Stan, M. Swierczynski, D.I. Stroe, R. Teodorescu, S.J. Andreasen, “Lithium ion Battery Chemistries from Renewable Energy Storage to Automotive and Back-up Power Applications – An Overview,” IEEE-OPTIM 2014, pp. 713-720, 22-25 May 2014.

[4] P.C. Kjær, R. Lærke, G. Tarnowski, ”Ancillary Services provided from Wind Power Plant Augmented with Energy Storage,” Power Electronics and Applications (EPE), 2013 15th European Conference on, pp. 1-7, 2-6 Sept. 2013.

[5] N. Omar et al., "Evaluation of performance characteristics of various lithium-ion batteries for use in BEV application," Vehicle Power and Propulsion Conference (VPPC), 2010 IEEE, pp.1-6, 1-3 Sept. 2010.

[6] D. Andre et. al., “Characterization of high-power lithium-ion batteries by electrochemical impedance spectroscopy. I. Experimantal investigation,” Journal of Power Sources, vol. 196, pp. 5534-5341, 2011.

[7] S. Buller, M. Thele, R. De Doncker, E. Karden, “Impedance-based simulation models of supercapacitors and Li-ion batteries for power electronic applications,” Industry Applications, IEEE Transactions on, vol. 41, pp.742-747, May-June 2005.

[8] B.V. Ratnakumar, M.C. Smart, L.D. Whitcanack, R.C. Ewell, “The impedance charcateristic of Mars Exploration Rover Li-ion batteries,” Journal of Power Sources, vol. 159, pp. 1428-1439, 2006.

[9] D.I. Stroe, M. Swierczynski, A.I. Stan, R. Teodorescu, S.J. Andreasen, “Experimentla Investigation on the Internal Resistance of Lithium Iron Phosphate Battery Cells during Calendar Ageing,” IEEE-IECON 2013 -, pp.6734-6739, 10-13 Nov. 2013.

[10] M. Ecker et al., ”Development of a lifetime prediction model for lithium-ion batteries based on extended accelerated ageing test data,” Journal of Power Sources vol. 215, pp. 248-257, 2012.

[11] H.-G. Schweiger et al., “Comparison of Several Methods for Determining the Internal Resistance of Lithium Ion Cells,” Sensors, vol. 10, pp. 5604-5625, 2010.

[12] E. Barsoukov and J.R. Macdonald, “Impedance Spectroscopy. Theory, Experiment and Applications,” Wiley 2005.

[13] W. Liu, C. Delacourt, C. Forgez, and S. Pelissier, “Study of graphite/nca li-ion cell degradation during accelerated aging tests - data analysis of the simstock project,” in IEEE-VPPC, pp. 1–6, 2011.

[14] J. Christophersen et al., “Electrochemical impedance spectroscopy testing on the advanced technology development program lithium-ion cells,” in Vehicular Technology Conference, Proceedings of 2002 IEEE 56th, vol. 3, 2002, pp. 1851–1855 vol.3.

[15] M.C. Smart et al., “Life verification of large capacity Yardney Li-ion cells and batteries in support of NASA missions,” International Journey of Energy Research, vol. 34, pp. 116-132, 2010.

[16] ISO 12405-1:2011, “Electrically propelled road vehicles – Test specification for lithium-ion traction battery packs and systems” 2011.

[17] D.I. Stroe, M. Swierczynski, A.I. Stan, V.Knap, R. Teodorescu, S.J. Andreasen, “Diagnosis of Lithium-Ion Batteries State-of-Health based on Electrochemical Impedance Spectroscopy Technique,” IEEE-ECCE 2014, pp.4576-4582, 14-18 Sep. 2013.